JOURNAL OF COMPUTATIONAL PHYSICS 70, 193–202 (1987)

Numerical Solutions for the Incompressible Navier–Stokes Equations in Primitive Variables Using a Non-staggered Grid, II

S. ABDALLAH

Applied Research Laboratory, The Pennsylvania State University, P.O. Box 30, State College, Pennsylvania 16804

Received November 11, 1985; revised August 4, 1986

In Part I of this study, a method was developed for the solution of the pressure Poisson equation, with Neumann boundary conditions, on a non-staggered grid. This method was used to determine the pressure when given the velocity field from a stream function–vorticity solution. In Part II, the pressure equation is solved iteratively with the momentum (Navier–Stokes) equations on a non-staggered grid. In this case, the solution of the pressure equation not only provides the pressure, but also serves to indirectly satisfy the continuity equation. This primitive variables formulation has a major advantage over the stream function–vorticity method in its applicability for three-dimensional flow. Numerical results are obtained and compared with the stream function–vorticity results for the driven cavity of Part I.

INTRODUCTION

Two methods are well known for the soution of the Incompressible Navier–Stokes equations in primitive variables; the artificial compressibility method and the pressure Poisson equation method.

In the artificial compressibility method, which was first suggested by Chorin [1], the time derivative of the pressure divided by a large constant is added to the continuity equation. The addition of the time-derivative term to continuity allows the use of standard compressible flow techniques for the incompressible equations. Choi and Merkle [2] investigated the stability and convergence characteristics of an implicit method for this system of equations. They recommended that the constant of the time derivative term in the continuity equation be chosen near the free-stream velocity to speed convergence of the numerical solutions (steady-state solutions only). Rizzi and Eriksson [3] examined the same system of equations and arrived at similar conclusions.

The pressure Poisson equation approach has been developed by Harlow and Welch in 1965 [4]. In their formulation, the unsteady momentum equation is solved for the velocity field by marching in time. The pressure is calculated from a

0021-9991/87 $3.00

discrete Poisson-type equation derived from the discrete divergence of the discrete momentum equation. The Poisson equation replaces the continuity equation which is satisfied indirectly through the solution of the pressure equation. Neumann boundary conditions are obtained for the pressure by using the momentum equation at the boundaries. As was discussed in Part I of this study, solutions for the Poisson equation with Neumann boundary conditions require the satisfaction of a compactibility condition. The new method we proposed in Part I satisfies this condition on non-staggered grids.

In the present study, numerical solutions are obtained for the Navier–Stokes equations on a non-staggered grid. The parabolic momentum equation is solved for the velocity field by marching in time using the simple explicit approach, while the elliptic pressure equation is solved at each time step using the successive-over-relaxation method. Although the calculations presented here are for steady-state flow, the method is valid for both steady and unsteady flow solutions. Details of the method are outlined in the following sections.

Mathematical Formulation

The momentum and continuity equations for incompressible laminar flow are written in Cartesian coordinates x and y.

The x-momentum equation is

$$u_t + uu_x + vu_y = -P_x + \frac{1}{\mathrm{Re}} (u_{xx} + u_{yy}). \tag{1}$$

The y-momentum equation is

$$v_t + uv_x + vv_y = -P_y + \frac{1}{\mathrm{Re}} (v_{xx} + v_{yy}). \tag{2}$$

The continuity equation is

$$u_x + v_y = 0. \tag{3}$$

In Eqs. (1)–(3), P, u, and v are the static pressure, velocity component in the x-direction, and velocity component in the y-direction, respectively. Re is the Reynolds number.

The momentum equations (1) and (2) are solved for the velocity components u and v, respectively, by marching in time. The pressure P is calculated from a Poisson-type equation which is derived from the momentum equations (1) and (2).

By differentiating Eq. (1) w.r.t x and Eq. (2) w.r.t y and adding, one obtains

$$P_{xx} + P_{yy} = \sigma - D_t, \tag{4}$$

where

$$\sigma = -(uu_x + vu_y)_x - (uv_x + vv_y)_y \tag{4a}$$

and

$$D = u_x + v_y. \tag{4b}$$

Equation (4) is a second order elliptic partial differential equation of the Poisson type. It is explicitly independent of the Reynolds number, because the diffusion terms are eliminated by the continuity equation. Aside from the unsteady term D_t, Eq. (4) for the static pressure is similar to Eq. (4) of Part I of this study. The dilation D is not present in Eq. (4) of Part I because the continuity equation is identically satisfied by the stream function–vorticity formulation. The governing equations (1)–(4) for the variables u, v, and P are not independent. The continuity equation (3) is eliminated from the system of equations, and it is iteratively satisfied through the solution of the pressure Eq. (4) as follows:

The unsteady term D_t in Eq. (4) is approximated by [4, 5],

$$D_t = \frac{D^{n+1} - D^n}{\Delta t}, \tag{4c}$$

where the superscripts n and $n+1$ refer to the time levels t and $t + \Delta t$, respectively.

In order to attempt to satisfy the continuity equation (3), D^{n+1} is set equal to zero. D^n is retained in Eq. (4c) to overcome nonlinear instabilities in the solution of the momentum equations (1) and (2) [4, 5]. Supporting evidence for the above arguments is given in the numerical solutions section.

Boundary Conditions

Referring to Fig. 1 of Part I, the following boundary conditions for Eqs. (1), (2), and (4) are adopted,

$$u = 0 \quad \text{at} \quad x = (0, 1) \text{ and } y = 0 \tag{5a}$$

$$u = 1 \quad \text{at} \quad y = 1 \tag{5b}$$

$$v = 0 \quad \text{at} \quad x = (0, 1) \text{ and } y = (0, 1) \tag{5c}$$

$$-P_x = uu_x + vu_y + \frac{1}{\text{Re}}\,\omega_y \quad \text{at} \quad x = (0, 1) \tag{6a}$$

$$-P_y = uv_x + vv_y - \frac{1}{\text{Re}}\,\omega_x \quad \text{at} \quad y = (0, 1), \tag{6b}$$

where

$$\omega = v_x - u_y. \tag{6c}$$

Equation (6) are Neumann-type boundary conditions for the pressure. The diffusion terms in Eq. (6) are written in terms of the vorticity ω following the method of Part I.

Existence and uniqueness of a solution to the pressure Poisson equation (4) and the Neumann boundary conditions (6) require the satisfaction of Eqs. (6) and (7) of Part I.

Numerical Solutions

The governing equations (1), (2), and (4) are approximated on a non-staggered grid with grid increments $\Delta x = \Delta y = h$. All the spatial derivatives in Eqs. (1), (2), and (4) are approximated using second order accurate finite-difference formulas.

Finite-Difference Approximations for Eqs. (1) and (2)

The time derivative terms in Eqs. (1) and (2) are approximated using forward time differences,

$$u^{n+1} = u - \frac{\Delta t}{2h}\left[u_{i,j}(u_{i+1,j} - u_{i-1,j}) + v_{i,j}(u_{i,j+1} - u_{i,j-1}) + P_{i+1,j} - P_{i-1,j}\right] + \Delta t(u_{i+1,j} + u_{i-1,j} + u_{i,j+1} + u_{i,j-1} - 4u_{i,j})/h^2 \mathrm{Re} \tag{7a}$$

$$v^{n+1} = v - \frac{\Delta t}{2h}\left[u_{i,j}(v_{i+1,j} - v_{i-1,j}) + v_{i,j}(v_{i,j+1} - v_{i,j-1}) + P_{i,j+1} - P_{i,j-1}\right] + \Delta t(v_{i+1,j} + v_{i-1,j} + v_{i,j+1} + v_{i,j-1} - 4v_{i,j})/h^2 \mathrm{Re}. \tag{7b}$$

The right-hand sides of the above equations are computed at the time level n.

It is interesting to note here that the final form of Eq. (4) (after enforcing $D^{n+1} = 0$) can be obtained by direct substitution of Eqs. (7) into Eq. (3) [6]. This confirms the development thta led to the pressure Poisson equation (4). The continuity equation is satisfied in continuum form in Eq. (4) (similar to the ψ–ω formulation).

Finite-Difference Approximation for Eq. (4)

Following the method of Part I for the solution of the pressure Poisson equation and referring to Fig. 2 of Part I, one obtains

$$\begin{aligned}(P_x)_e - (P_x)_w + (P_y)_n - (P_y)_s &= (uu_x + vu_y)_w - (uu_x + vu_y)_e + (uv_x + vv_y)_s \\ &\quad - (uv_x + vv_y)_n + (u_e - u_w + v_n - v_s)/\Delta t.\end{aligned} \tag{8}$$

At the locations e, w, n, and s, the variables in Eq. (8) are approximated from the variables at the grid points by averaging. For example, at the location e,

$$(uu_x)_e = (u_{i+1,j} + u_{i,j})(u_{i+1,j} - u_{i,j})/2h \tag{9a}$$

$$(vu_y)_e = (v_{i+1,j} + v_{i,j})(u_{i+1,j+1} + u_{i,j+1} - u_{i+1,j-1} - u_{i,j-1})/4h \tag{9b}$$

$$(u)_e = (u_{i+1,j} + u_{i,j})/2. \tag{9c}$$

Similar expressions are obtained at the locations w, n, and s. By substituting these relations in Eq. (8), one obtains

$$\begin{aligned} P_{i+1,j} &+ P_{i-1,j} + P_{i,j-1} P_{i,j+1} - 4P_{i,j} \\ &= h\sigma_{i,j} + (u_{i+1,j} - u_{i-1,j} + v_{i,j+1} - v_{i,j-1})\, h/2\Delta t, \end{aligned} \tag{10a}$$

where

$$\begin{aligned} -\sigma_{i,j} = {} & (u_{i+1,j} + u_{i,j})(u_{i+1,j} - u_{i,j})/2 + (v_{i+1,j} + v_{i,j})(u_{i+1,j+1} \\ & + u_{i,j+1} - u_{i+1,j-1} - u_{i,j-1})/8 - (u_{i,j} + u_{i-1,j})(u_{i,j} - u_{i-1,j})/2 \\ & - (v_{i,j} + v_{i-1,j})(u_{i,j+1} + u_{i-1,j+1} - u_{i,j-1} - u_{i-1,j-1})/8 \\ & + (u_{i,j+1} + u_{i,j})(v_{i+1,j+1} + v_{i+1,j} - v_{i-1,j+1} - v_{i-1,j})/8 \\ & + (v_{i,j+1} + v_{i,j})(v_{i,j+1} - v_{i,j})/2 - (u_{i,j} + u_{i,j-1})(v_{i+1,j} \\ & + v_{i+1,j-1} - v_{i-1,j} - v_{i-1,j-1})/8 - (v_{i,j} + v_{i,j-1})(v_{i,j} - v_{i,j-1})/2. \end{aligned} \tag{10b}$$

Finite-difference approximations for the pressure Neumann boundary conditions (6) are obtained at the grid locations $i = (\frac{3}{2}, M - \frac{1}{2})$ and $j = (\frac{3}{2}, N - \frac{1}{2})$ (see Part I). M and N are the number of grid points in the x- and y-directions, respectively,

$$\begin{aligned} P_{2,j} - P_{1,j} = {} & -(\omega_{2,j+1} + \omega_{1,j+1} - \omega_{2,j-1} - \omega_{1,j-1})/4\,\mathrm{Re} \\ & - (u_{2,j} + u_{1,j})(u_{2,j} - u_{1,j})/2 - (v_{2,j} + v_{1,j}) \\ & \times (u_{2,j+1} + u_{1,j+1} - u_{2,j-1} - u_{1,j-1})/8 \qquad (2 \leqslant j \leqslant N-1) \end{aligned} \tag{11a}$$

$$\begin{aligned} P_{M,j} - P_{M-1,j} = {} & -(\omega_{M,j+1} + \omega_{M-1,j+1} - \omega_{M,j-1} - \omega_{M-1,j-1})/4\,\mathrm{Re} \\ & - (u_{M,j} + u_{M-1,j})(u_{M,j} - u_{M-1,j})/2 - (v_{M,j} + v_{M-1,j}) \\ & \times (u_{M-1,j+1} + u_{M,j+1} - u_{M-1,j-1} - u_{M,j-1})/8 \qquad (2 \leqslant j \leqslant N-1) \end{aligned} \tag{11b}$$

$$\begin{aligned} P_{i,2} - P_{i,1} = {} & (\omega_{i+1,2} + \omega_{i+1,1} - \omega_{i-1,2} - \omega_{i-1,1})/4\,\mathrm{Re} \\ & - (u_{i,2} + u_{i,1})(v_{i+1,2} + v_{i+1,1} - v_{i-1,2} - v_{i-1,1})/8 \\ & - (v_{i,2} + v_{i,1})(v_{i,2} - v_{i,1})/2 \qquad (2 \leqslant i \leqslant M-1) \end{aligned} \tag{11c}$$

$$P_{i,N} - P_{i,N-1} = (\omega_{i+1,N} + \omega_{i+1,N-1} - \omega_{i-1,N} - \omega_{i-1,N-1})/4\,\mathrm{Re}$$
$$- (u_{i,N} + u_{i,N-1})(v_{i+1,N-1} + v_{i+1,N} - v_{i-1,N-1})/8$$
$$- (v_{i,N} + v_{i,N-1})(v_{i,N} - v_{i,N-1})/2 \qquad (2 \leqslant i \leqslant M-1). \tag{11d}$$

Note that

$$u_{1,j} = u_{M,j} = v_{1,j} = v_{M,j} = 0 \qquad (1 \leqslant j \leqslant N) \tag{12a}$$
$$u_{i,1} = v_{i,1} = v_{i,N} = 0 \qquad (1 \leqslant i \leqslant M) \tag{12b}$$
$$u_{i,N} = 1 \qquad (1 \leqslant i \leqslant M). \tag{12c}$$

Results and Discussion

Equation (10) is solved for the pressure using the successive over-relaxation method (SOR). The continuity equation is implied at each grid point in the solution of Eq. (10). Then the velocity components u^{n+1} and v^{n+1} are obtained from Eqs. (7a) and (7b), respectively. The explicit marching procedure is used here for the solution of the momentum equations for simplicitly.

For steady-state flow, the transient solutions of Eqs. (7) and (10) are not physically meaningful, and consequently Eq. (10) need not be iterated to full convergence at each time step (few iterations are necessary for smooth results). However, for unsteady flow the pressure equation (10) be iterated to full convergence at each time step (in order to satisfy the continuity equation) before marching to the next time level.

Numerical results are obtained for the driven cavity used in Part I of this study and shown in Fig. 1 of Part I. The computed results at Re = 100 using 41 × 41 grid points are compared with the results of Part I of this study. It can be seen from Figs. 1, 2, and 3 that the vorticity, static pressure, and total pressure contours com-

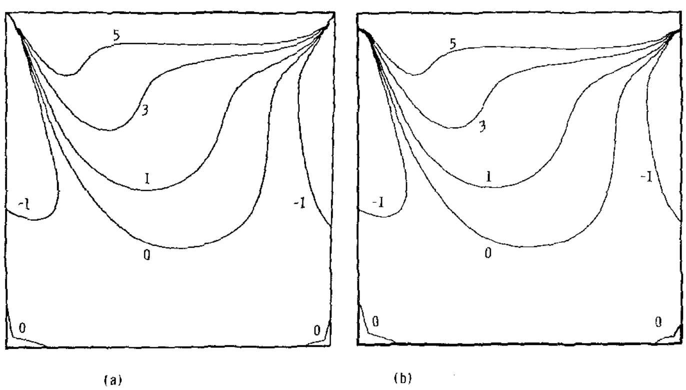

FIG. 1. Vorticity contours at Re = 100. (a) ψ–ω formulation, (b) primitive variables formulation.

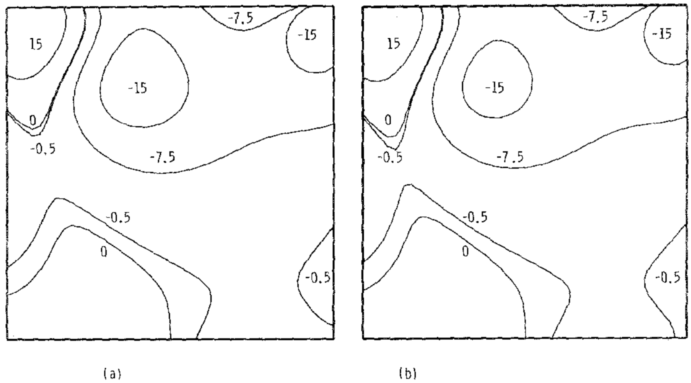

FIG. 2. Static pressure contours ($\mathrm{Re}\,C_{p_s}$) at Re = 100. (a) ψ–ω formulation, (b) primitive variables formulation.

puted using the primitive variable formulation are in excellent agreement with the results of the stream function–vorticity approach. The static and total pressure coefficients are defined in Part I of this study.

Additional results are obtained in Figs. 4, 5, and 6 at Re = 400, using 71×71 grid points. The computed results are compared with the numerical results of Ref. [7] which employed the stream function–vorticity fomulation. All calculations are obtained using a successive over relaxation factor 1.0 and a time increment $\Delta t = 0.012$. The explicit time increment is governed by [5] $\Delta t/h < 1$ and $\Delta t/h^2 \mathrm{Re} < \frac{1}{4}$. A detailed comparison between the primitive variable and the stream function-vorticity formulations is given in Table I.

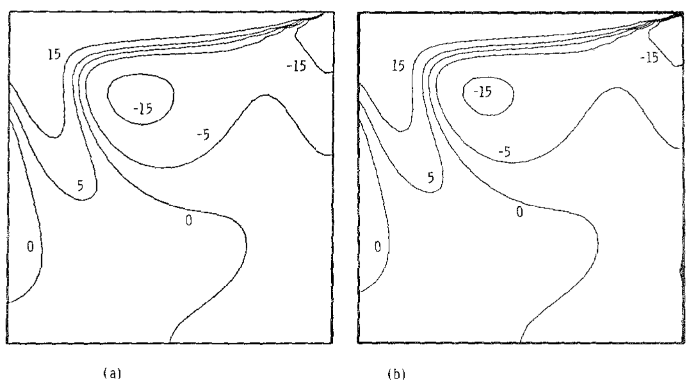

FIG. 3. Total pressure contours ($\mathrm{Re}\,C_{p_t}$) at Re = 100. (a) ψ–ω formulation, (b) primitive variables formulation.

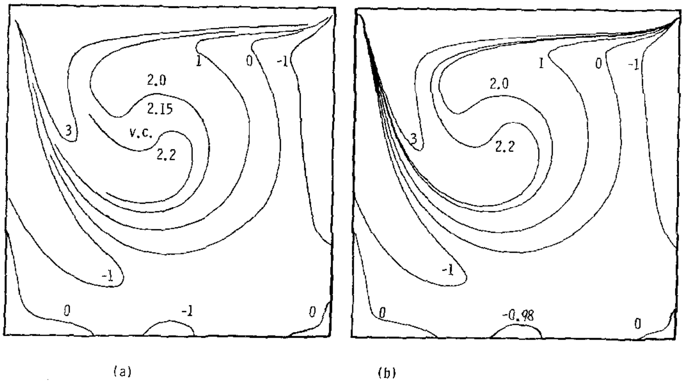

FIG. 4. Vorticity contours at Re = 400. (a) ψ–ω formulation, (b) primitive variables formulation.

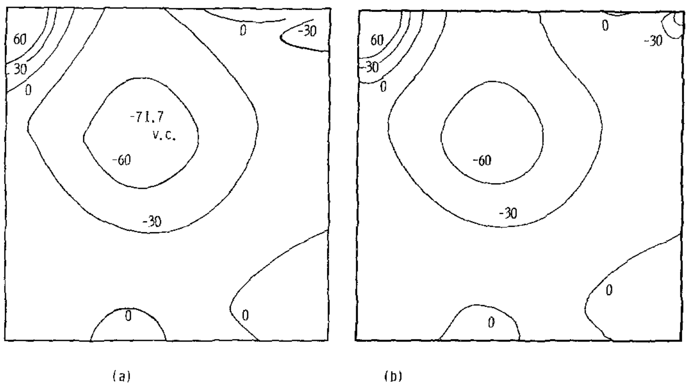

FIG. 5. Static pressure contours ($\mathrm{Re}\,C_{p_s}$) at Re = 400. (a) ψ–ω formulation, (b) primitive variables formulation.

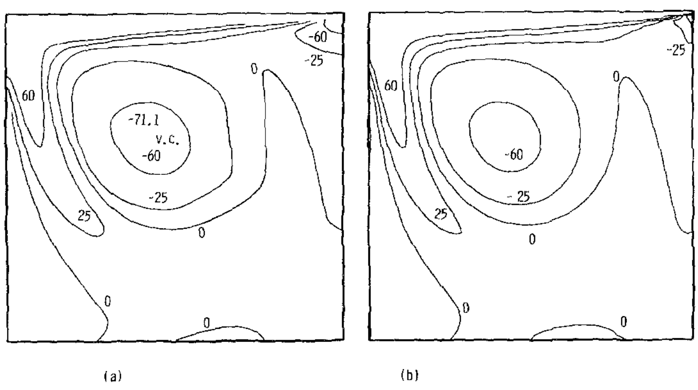

FIG. 6. Total pressure contours ($\mathrm{Re}\,C_{p_t}$) at Re = 400. (a) ψ–ω formulation, (b) primitive variables formulation.

TABLE I

Type	Primitive variables	Stream function–vorticity
Dependent variables	the dependent variables are the velocity and the pressure	the dependent variables are the stream function, the vorticity, and the pressure
Governing equations	the governing equations are the momentum and the pressure Poisson equation	the governing equations are the stream function, the vorticity-transport, and the pressure Poisson equation
Method of solution	the momentum equations are solved using the explicit approach. While the pressure equation is solved using the SOR method	the governing equations are solved using the SOR method
Continuity equation	the continuity equation is replaced and indirectly satisfied by the pressure Poisson equation	the continuity equation is identically satisfied by the use of a stream function
Pressure equation	the pressure equation is solved iteratively at each time step (few iterations are anecessary for smooth results; 10 iterations are used here)	the pressure equation is uncoupled from the stream function and vorticity equations. It is solved after the velocity field is computed
Boundary conditions	the boundary conditions for the momentum equations are the no-flux and no-slip conditions. Neumann boundary conditions for the pressure are obtained from the momentum equations	the boundary conditions for the stream function and the vorticity are obtained from the no-slip and no-flux conditions. Neumann boundary conditions of the pressure are obtained from the momentum equations

CONCLUSIONS

Numerical solutions for the incompressible Navier–Stokes equations in primitive variables are obtained on non-staggered grids. The primitive variable formulation has a major advantage over the stream function–vorticity method in its applicability for three-dimensional flow. In Part II the pressure and velocity equations are solved at each time step, which leads to an extra dilation term in the pressure Poisson equation. This additional term causes no problem in the compatibility condition because the integral of the dilation over the solution domain vanishes (from the global continuity). Thus the method developed in Part I is used for the solution of the pressure Poisson equation without modification. The computed results using the primitive variable formulation are in excellent agreement with the results of the stream function–vorticity method.

APPENDIX: NOMENCLATURE

D	dilation Eq. (4b)
h	grid spacing
M, N	number of grid points in x- and y-directions, respectively
P	static pressure
S	boundary contour enclosing the solution domain
u, v	velocity components in x- and y-directions, respectively
U	velocity of the cavity upper wall
dS	increment along the boundary contour S
LHM, RHM	summation of the left- and right-hand members of the compatibility condition
Re	Reynolds number
σ	right-hand side of Eq. (4)
ω	vorticity

Subscripts

e, w, n, s	refer to east, west, north, and south of the grid points (i, j), respectively
n	refers to the outward normal to the boundary contour S
x, y	refer to partial derivatives with respect to x and y, respectively
i, j	refer to grid locations in x- and y-directions, respectively

ACKNOWLEDGMENT

This work was sponsored by the U.S. Office of Naval Research.

REFERENCES

1. A. J. CHORIN, *J. Comput. Phys.* **2**, 12 (1967).
2. D. CHOI AND C. L. MERKLE, *AIAA J.* **23**, 1518 (1985).
3. A. RIZZI AND L. ERIKSSON, *J. Fluid Mech.* **163**, 275 (1985).
4. F. H. HARLOW AND J. E. WELCH, *Phys. Fluids* **8**, 2182 (1965).
5. P. J. ROACHE, *Computational Fluid Dynamics* (Hermosa, Albuquerque, NM, 1976), p. 194.
6. J. D. HUDSON AND S. C. R. DENNIS, *J. Fluid Mech.* **160**, 369 (1985).
7. O. R. BURGGRAF, *J. Fluid Mech.* **24**, 113 (1966).